Supplementary Information

Mechanistic insight into the role of aspect ratio of nanofillers for gas barrier properties in polymer nanocomposite thin films

[1,2]Subhash Mandal, [2]Debmalya Roy*, [2]Kingsuk Mukhopadhyay, [3]Mayank Dwivedi and [1]Mangala Joshi*

[1]Indian Institute of Technology Delhi, Hauz Khas, New Delhi-110016.
[2]Directorate of Nanomaterials and Technologies (DNMAT), Defence Materials and Stores Research & Development Establishment (DMSRDE), DRDO, G T Road, Kanpur-208013, India.
[3]DMSRDE, DRDO, G T Road, Kanpur-208013, India.
E-mail: *mangala@textile.iitd.ac.in; mangalajoshi9@gmail.com; #droy.dmsrde@gov.in

S1. THEORY OF GAS PERMEABILITY: MECHANISM, MEASUREMENT AND MODELLING

S1.1. The gas transport mechanism in polymer films and polymer nanocomposite membranes.

The process of gas transport through polymer membranes or films is a multifaceted phenomenon. Initially, the gas molecules either adhere to the surface of the membrane/film or dissolve within it before proceeding to diffuse through. During the adsorption phase on amorphous polymeric materials, gas molecules occupy the vacant spaces created by the thermal motion of polymer chains or Brownian motion. Subsequently, during diffusion, these gas molecules navigate through the interconnected free spaces within the polymer structure. Thus, the effectiveness of diffusion relies on the size and quantity of these free spaces within the polymer. The rate of gas diffusion is influenced by the dynamic free volume generated by the segmental movement of the polymer chains, while the solubility of gases is affected by the interactions between the gas molecules and the polymeric chains [1, 2].

In the case of semicrystalline polymeric membranes or films, factors such as the size, shape, structure, orientation, and degree of crystallinity of the crystallites play a pivotal role in the gas permeation process. Polyurethane (PU), for instance, is a semicrystalline polymer with a minimal fraction of crystalline segments or hard segments. As the proportion of soft segments in PU increases, more free volume is created, resulting in an enhanced rate of gas diffusion through PU films/membranes. In terms of gas permeation, polymer nanocomposites exhibit behavior akin to semicrystalline polymers [3]. In gas barrier polymer nanocomposites,

impermeable nano-platelets are dispersed within a polymer matrix, impeding the diffusion of gas molecules by forcing them to traverse a more intricate path. In contrast, micro-additive-reinforced polymeric composites are less effective in enhancing the gas barrier properties of the polymer, as shown in Figure S1.

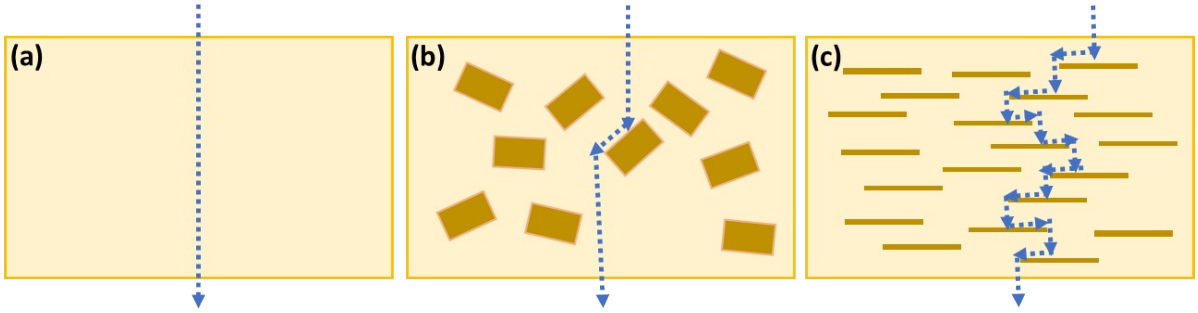

Figure S1: *Gas permeation through three scenarios: (a) polymer alone, (b) polymer with micro-fillers, and (c) polymer nanocomposite.*

One of the most widely accepted theories explaining gas transmission through nonporous polymeric barriers is the activated diffusion mechanism. The rate of gas transmission via the activated diffusion mechanism is influenced by several factors, including the type of plastic used, temperature, humidity, and the size of the gas molecules in motion [4]. The amount of gas flow is directly proportional to the fourth power of the size of any openings in the material. Typically, the gas flow rate also depends on the number of such openings and the pressure difference between the two sides of the film [5]. Intriguingly, Madhavan et al. [6] observed that the permeabilities of nitrogen (N_2) and oxygen (O_2) through poly(dimethylsiloxane)-urethane (PDMS-PU) membranes were not influenced by pressure, whereas CO_2 permeability increased with pressure. Another study [7] reported that N_2 and O_2 permeabilities of all PDMS-PU and polypropylene glycol-PU (PPGPU) membranes decreased as the pressure of the penetrating gases increased. The compression of the polymer matrix under higher pressure might be responsible for reducing the available free volume for gas diffusion, resulting in reduced permeabilities. Generally, the gas flow rate is inversely proportional to the viscosity of the gas and the thickness of the film [8-10].

S1.2. The process of measuring gas permeability across polymeric membranes or films.

Gas permeation through a polymeric membrane or film involves a complex process with three fundamental steps [3]:

Adsorption: Gas molecules initially adhere to the surface of the membrane or film.

Diffusion: Gas molecules then traverse through the membrane or film.

Desorption: Finally, gas molecules detach from the opposite surface of the membrane or film. The theories governing gas transmission through polymeric films or membranes are based on diffusion models related to Henry's and Fick's laws [11-13]. Figure 2 depicts diffusion through a uniform-thickness polymeric film or membrane, where the permeant concentration is represented as 'c' (with 'c1' and 'c2' denoting higher and lower permeant concentrations, respectively, where c1 > c2), and the permeant pressure is 'p' (with 'p1' and 'p2' indicating higher and lower permeant pressures, respectively, where p1 > p2).

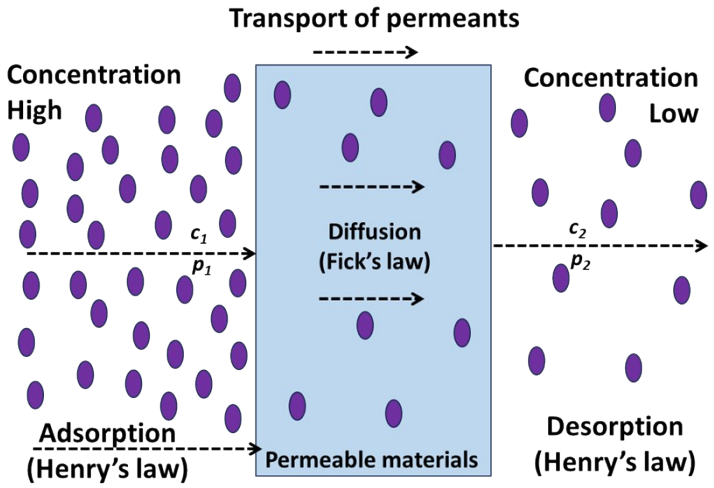

Figure S2: *Schematic depicting the gas permeation process through a polymeric film, with "c" and "p" denoting the concentration and pressure of the diffusing gas or permeant (where $c_1 > c_2$ and $p_1 > p_2$).*

According to Fick's first law [13]:

$$J = -\ D.\frac{\Delta c}{l} \quad \text{----------(S1)}$$

Here, 'J' represents the permeant (gas or vapor) flux (in $mol.cm^{-2}.s^{-1}$), 'D' is the diffusion constant (in $cm^2.s^{-1}$), 'Δc' denotes the concentration difference (in mol/cm^3) across the film or membrane of thickness 'l' (in cm).

In a steady-state condition, both 'c' and 'p' adhere to Henry's law. Nevertheless, it is often more practical to measure gas pressure 'p' rather than concentration 'c'. By substituting 'Δc' with 'Δp', we obtain:

$$J = -\ D.(\frac{s\Delta p}{l}) \quad \text{----------(S2)}$$

Where 'Δp' (in atm) signifies the pressure difference across the film or membrane, and 'S' represents the solubility or sorption coefficient (in $mol.cm^{-3}.Pa^{-1}$), indicating the quantity of permeant present in the polymer.

If 'S' remains independent of concentration, the gas permeability coefficient, denoted as 'P' (in mol.Pa^{-1}.cm^{-1}.s^{-1}), can be expressed as follows:

$$P = -\frac{J.i}{\Delta p} = D.S \quad \text{----------(S3)}$$

The ratio of 'P/l' is commonly referred to as 'q' and is known as permeance. This kind of diffusion, where 'D' and 'S' do not depend on permeant concentration, is termed Fickian behavior [11]. However, in some cases, gas molecule diffusion behavior is contingent on permeant concentration, a phenomenon referred to as non-Fickian behavior. This occurs when interactions take place between polymers and permeants, such as the interaction between water vapor and a hydrophilic film [12].

The gas permeability of a membrane or film can be determined through direct measurements in a cell or indirect sorption/desorption experiments. In direct measurements, the membrane or film divides the cell into two compartments. Gas is introduced on one side while maintaining a constant pressure. Gas flux density in the other compartment is monitored, with the gas permeability coefficient recorded once it reaches a steady-state distribution [3]. Alternatively, a Wicke-Kallenbach device can be employed. In this method, a gas mixture like CO_2 and N_2 is introduced on one side, while a reference gas like N_2 is maintained on the other side, and the permeation of the test gas (CO_2) is measured with equal pressure in both compartments [13]. Gas selectivity is determined by comparing the permeabilities of the two gases.

In sorption/desorption experiments, both the diffusion coefficient and the solubility coefficient are measured, and gas permeability is determined using Equation (S3). Initially, the membrane is under vacuum, and then gas is introduced at a constant pressure. Gas dissolves and diffuses into the membrane or film, with the weight gain tracked over time using a balance. The diffusion coefficient is calculated based on a specific formula, assuming a uniform gas distribution in a flat membrane with thickness 'd'. Meanwhile, the solubility coefficient is determined by measuring the concentration of a soluble gas as a function of pressure [14]. Various models have been proposed by researchers to calculate permeability by assessing the diffusion coefficient and solubility, which will be discussed in detail later on.

S1.3.1 Influence of Nanoplatelets' Volume Fraction and Aspect Ratio

Eitzman et al. [15] devised an approximate derivation of Cussler's equation tailored for barrier membranes housing tipped flakes. This theoretical framework was constructed through Monte Carlo simulations, incorporating the influence of flake orientation, and is expounded as follows:

$$\frac{P}{P_0} = \frac{1-\phi}{\alpha^2\phi^2 Cos^2\theta}$$ ---------- (S4)

In this context, θ represents the angle of orientation of the flakes in degrees. Expanding upon the analogous flake-filled membrane framework, Falla et al. [16] introduced two additional adaptations of Cussler's model. These adaptations are analogous to Aris' model [17] and the Wakeham-Mason model [18], and they are formulated as Eq. (S5) and Eq. (S6) respectively.

$$\frac{P}{P_0} = \left(1 + \frac{\alpha^2\phi^2}{1-\phi} + \frac{\alpha\phi}{\sigma} + \frac{4\alpha\phi}{\pi(1-\phi)}\ln\left[\frac{\pi\alpha^2\phi}{\sigma(1-\phi)}\right]\right)^{-1}$$ ---------- (S5)

$$\frac{P}{P_0} = \left(1 + \frac{\alpha^2\phi^2}{1-\phi} + \frac{\alpha\phi}{\sigma} + 2(1-\phi)\ln\left[\frac{1-\phi}{2\sigma\phi}\right]\right)^{-1}$$ ---------- (S6)

Here, σ is defined as σ = s/a, representing the slit shape parameter. Eq. (S5) and Eq. (S6) exhibit a discrepancy in their fourth terms on the right-hand side. Aris Model's relative gas permeability is contingent upon the aspect ratio, whereas the Wakeham-Mason model does not display this dependency.

Lape and colleagues [19] introduced an altered model that accommodates rectangular-shaped flakes or nanoplatelets with the same aspect ratio. These flakes are positioned parallel to each other and oriented perpendicular to the direction of gas diffusion, yet arranged randomly. According to their proposed model:

$$\frac{P}{P_0} = \left(\frac{A_f}{A_0}\right).\left(\frac{l}{l'}\right)$$ ---------- (S7)

Here, A_f and A_0 denote the accessible diffusion areas within a flake-filled and uniform membrane, respectively. The parameter l signifies the distance traversed by gas molecules during diffusion within the polymer nanocomposite, and its expression is articulated as follows:

$$l' = l + N.d$$ ---------- (S8)

This equation corresponds to Eq. (4) in the main file, with the sole alteration being the substitution of L/2 with 'd', representing the average distance a gas molecule must traverse to reach the platelet's edge. By introducing certain assumptions, the value of 'd' can be estimated by considering that gas molecules randomly collide with platelets along their length, and the hindrance to mass transfer is proportionate to the distance travelled. Therefore, l' is transformed to:

$$l' = \left(1 + \frac{2}{3}\alpha\phi\right)l$$ ---------- (S9)

Equation (S9) deviates from Equation (4) in the main file by a factor of 2/3, attributable to the stochastic arrangement of nanoplatelet positions. The calculation of A_f involves dividing the accessible volume for diffusion by the distance covered through the membrane. Consequently, A_f can be computed as the ratio of the available diffusion volume to the distance traversed within the membrane. Therefore,

$$\frac{A_f}{A_0} = \frac{\frac{V_m - V_f}{l'}}{\frac{V_m}{l}} \quad \text{---------- (S10)}$$

Where V_f represents the cumulative volume of all nanoplatelets, and V_m signifies the overall volume of the membrane. As a result, the relative permeability can be expressed in the following manner:

$$\frac{P}{P_0} = \frac{1 - \phi}{\left(1 + \frac{2}{3}\alpha\phi\right)^2} \quad \text{---------- (S11)}$$

For a structured array of uniformly sized flakes, this equation simplifies to the following form:

$$\frac{P}{P_0} = \frac{1 - \phi}{(1 - \phi + \alpha^2\phi^2)} \quad \text{---------- (S12)}$$

In 1999, Fredrickson and Bicerano extended their modifications to both Nielsen's equation and the Cussler-Aris equations to encompass circular disk-like fillers, characterized by a radius R and thickness 2W [20]. These adapted equations offer an expanded scope across various φ ranges, catering to both dilute and semi-dilute conditions. The revised form of Nielsen's equation can be articulated as follows:

$$\frac{P}{P_0} = \frac{1}{1 + k\alpha\phi} \quad \text{---------- (S13)}$$

With $k = \pi/\ln\alpha$ and its relevance within the realm of sparse disk concentration ($\alpha\varphi << 1$), the modified Neilsen's equation demonstrates precision within the constraints of $k\alpha\phi \leq 3$. In a parallel manner, the 'modified Cussler-Aris' equation takes on the following expression:

$$\frac{P}{P_0} = \frac{1}{(1 + \mu\alpha^2\phi^2)} \quad \text{---------- (S14)}$$

For a semi-dilute scenario characterized by disk concentration (φ) significantly greater than 1 but with a constraint that $\alpha\varphi << 1$, a parameter $\mu = \pi^2/16\ln\alpha$ becomes relevant. In the context where $k\alpha\phi \geq 12$ [20, 21], the modified Cussler-Aris equation is known to hold true.

In the year 2001, Gusev and Lusti devised a computer model involving a three-dimensional periodic arrangement of multiple inclusions. This arrangement represents a random array of perfectly aligned circular discs [22]. The foundation of this model relies on solving the Laplace equation for the local chemical potential.

$$divP(r).grad\mu = 0 \quad \text{---------- (S15)}$$

The proposed model introduces a position-dependent local permeability coefficient denoted as P(r). This coefficient holds a value of zero within the platelets. The model's formulation is presented as follows:

$$\frac{P}{P_0} = exp\left[-\left(\frac{\alpha\phi}{x_0}\right)^{\beta}\right] \quad \text{---------- (S16)}$$

The values x_0 =3.47 and β=0.71 are typically determined through the process of fitting experimental data.

S1.3.2. Influence of nanoplatelet orientation

It has been observed that nanoplatelets are commonly found in a random arrangement within a polymer matrix [23]. Nevertheless, the gas barrier properties of polymer nanocomposites exhibit a significant correlation with the orientation of these nanoplatelets within the polymer matrix. Consequently, in an effort to incorporate the impact of nanoplatelet orientation on the gas permeability of polymer nanocomposites, Bharadwaj (2001) expanded upon the Nielsen's model. This expansion involved the introduction of an order parameter (S), which is defined as follows:

$$S = \frac{1}{2}(3cos^2\theta - 1) \quad \text{---------- (S17)}$$

In this context, the symbol θ denotes the angle existing between the preferred orientation direction (n) and the unit vector of the sheet's normal (p) [24]. When θ equals 0°, S takes on a value of 1, indicating a state of perfect alignment. In contrast, at θ of 90°, S becomes -1/2, signifying a perpendicular or orthogonal nanoplatelet orientation that leads to minimal hindrance for gas molecule diffusion within the nanocomposite. Furthermore, S equals 0 when θ reaches 54.74°, indicating a random nanoplatelet orientation within the polymer matrix [23, 24].

Based on Bharadwaj's model, the relative permeability of a polymer nanocomposite can be expressed as:

$$\frac{P}{P_0} = \frac{1-\phi}{1+\frac{\alpha}{2}*\frac{2}{3}\left(1+\frac{S}{2}\right)\phi} = \frac{1-\phi}{1+\frac{\alpha}{3}\left(1+\frac{S}{2}\right)\phi} \quad \text{----------} \quad \text{(S18)}$$

The provided equation simplifies to Equation (7)[in the main file] when S = 1, indicating a planar arrangement. In this scenario, the stacked layers of nanoplatelets in a horizontal manner induce a high level of tortuosity, leading to a notable reduction in the rate of gas permeation across polymer nanocomposites [3, 25].

Conversely, Equation (S6) approximately converges to the permeability of the pure polymer when S = −1/2, signifying an orthogonal arrangement.

Taking a distinct approach, Maksimov and colleagues [26] formulated an empirical relationship for quantifying moisture permeability within a polymer nanocomposite containing 3D nanoplatelets oriented in a random manner. This model can be expressed as follows:

$$P = \frac{1}{3}\left(P\| + 2P_0(1-\phi)\right) \quad \text{----------} \quad \text{(S19)}$$

The term "P‖" denotes the permeability of polymer nanocomposites, which is described by the Nielsen model for oriented nanoplatelets. Meanwhile, the subsequent component signifies the adjustment factor for the permeability of the nanocomposites, wherein the nanoplatelets are aligned in alignment with the direction of diffusion.

S1.3.3. Influence of the interfacial regions

In numerous instances, the presence of interfacial regions, which are established either through the application of surfactants during nanoplatelet modification or by the generation of gaps between two distinct phases, has an impact on gas permeability. Sorrentino et al. [27] formulated an equation to describe the relative diffusion coefficient as follows:

$$\frac{D_c}{D_m} = \frac{a'}{\tau} \quad \text{----------} \quad \text{(S20)}$$

Here, D_c and D_m represent the diffusion coefficients within the composite and the matrix, respectively. The parameter a' signifies a coefficient that measures the influence of the interfacial regions, and its computation is achieved as depicted below:

$$a' = 1 + \beta'\phi \quad \text{----------} \quad \text{(S21)}$$

This coefficient significantly shapes the diffusivity across all concentrations of the impermeable phase (filler). It can be formulated as follows:

$$\beta' = \frac{V_s}{V_f} * \frac{D_s}{D_0} - \frac{V_s + V_f}{V_f} \quad \text{---------- (S22)}$$

Here, D_s and D_0 denote the diffusion coefficients within the interfaces and the pure polymer, respectively. V_s and V_f stand for the volumes of the interfaces and the nanoplatelets, respectively. In scenarios where the ratio V_s/V_f holds negligible significance, β' assumes a value of -1 and α' becomes 1-ϕ. Nevertheless, it's worth noting that measuring the values of Vs and Ds poses considerable challenges [27].

S1.3.4. Influence of the state of delamination and the dispersion characteristics of nanoplatelets within the polymer matrix.

The anticipated enhancement in the gas barrier properties of polymer nanocomposites hinges significantly on the state of platelet delamination and the extent of nanoplatelet dispersion within the polymer matrix. However, the actual gas barrier property values predicted by the model often diverge from experimental outcomes, with a few exceptions, primarily due to the tendency of nanoplatelets to aggregate, especially at higher loadings [24, 28]. The effective width of nanoplatelets within polymer nanocomposites can exhibit variability contingent on the degree of delamination. As delamination increases, the nanoplatelets attain better exfoliation within the polymer matrix, constituting the pivotal factor for achieving maximal gas barrier performance in polymer nanocomposites.

Nonetheless, the aggregation of sheets or platelets leads to a pronounced reduction in tortuosity, facilitating the formation of percolating pathways for the diffusing gas [24]. Consequently, the relative permeability of a polymer nanocomposite progressively rises as the aggregate width increases.

S1.3.5. Influence of the number of layers in nanoplatelets and the phenomenon of their aggregation

Numerous sources have documented that as the number of layers in the stacking of nanoplatelets increases, the overall tortuosity of the polymer matrix diminishes, leading to heightened gas permeability across polymer nanocomposites. In light of this, Nazarenko et al. [29] made adjustments to Nielsen's equation to incorporate the influence of the number of disklike layers (N) within the stack resulting in the following modification:

$$\frac{P}{P_0} = \frac{1-\phi}{1+\frac{L\phi}{2hN}} = \frac{1-\phi}{1+\frac{\alpha\phi}{2N}}$$ ----------

(S23)

Here, 'h' signifies the thickness of the disk, and its relationship with the width of the stack (W) and the number of layers (N) is expressed as follows:

$W = hN + L(N-1)$ ---------- (S24)

Following that, a factor of 1/3 was introduced into the denominator when the aggregates were distributed in a random manner, resulting in the subsequent expression:

$$\frac{P}{P_0} = \frac{1-\phi}{\frac{1}{3}\left(1+\frac{\alpha\phi}{2N}\right)}$$ ----------

(S25)

When N equals 1, it signifies complete detachment of layers or thorough exfoliation, leading to the optimal gas barrier performance of polymer nanocomposites. In contrast, as the value of N increases significantly, the extent of layer detachment diminishes, yielding unsatisfactory gas barrier performance for polymer nanocomposites.

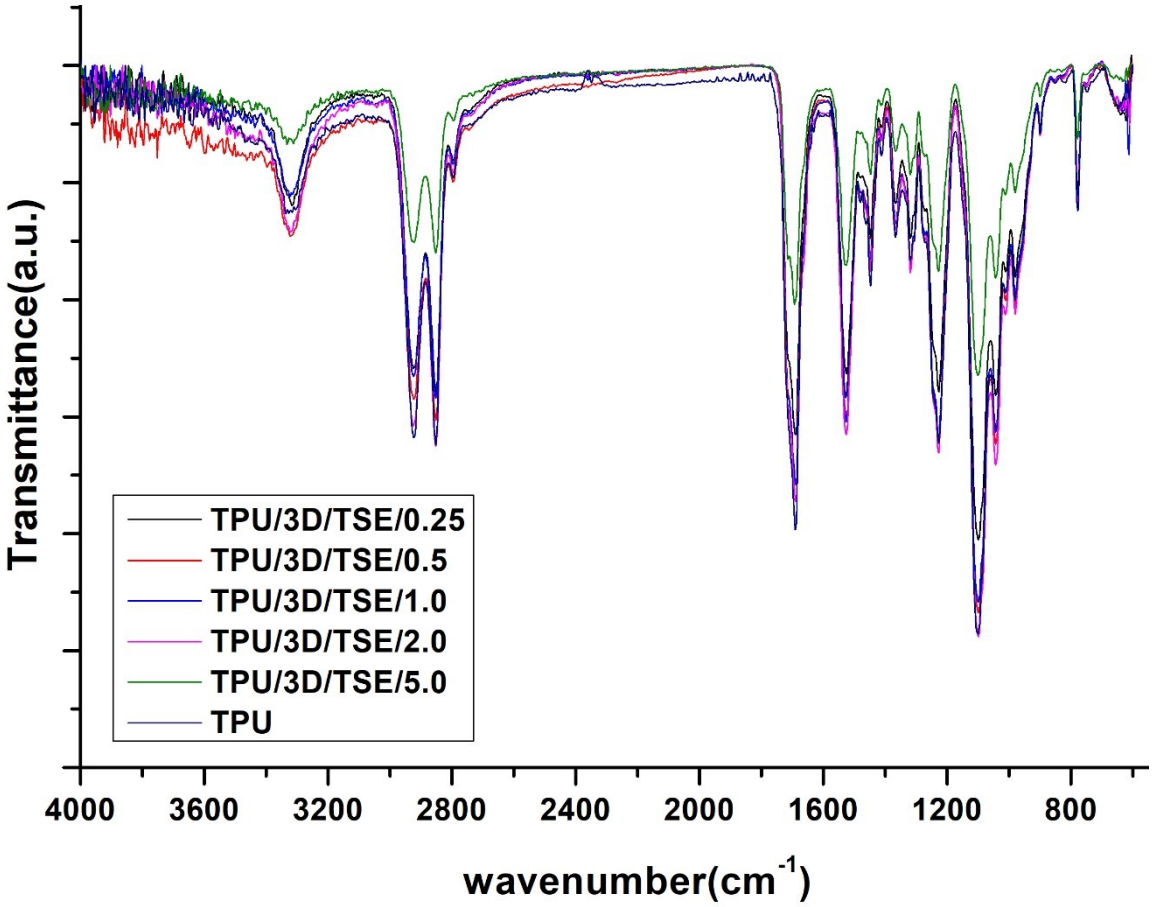

Figure S3: *ATR-FTIR spectra of neat thermoplastic polyurethane (TPU, navy blue color); polyurethane nanocomposite films reinforced with 0.25 wt% (TPU/3D/TSE/0.25, black color), 0.5 wt% (TPU/3D/TSE/0.5, red color), 1.0 wt% (TPU/3D/TSE/1.0, blue color), 2 wt% (TPU/3D/TSE/2.0, magenta color) and 5 wt% (TPU/3D/TSE/5.0, green color) hybrid 3D nanofillers by TSE in the range 4000-600 cm^{-1}.*

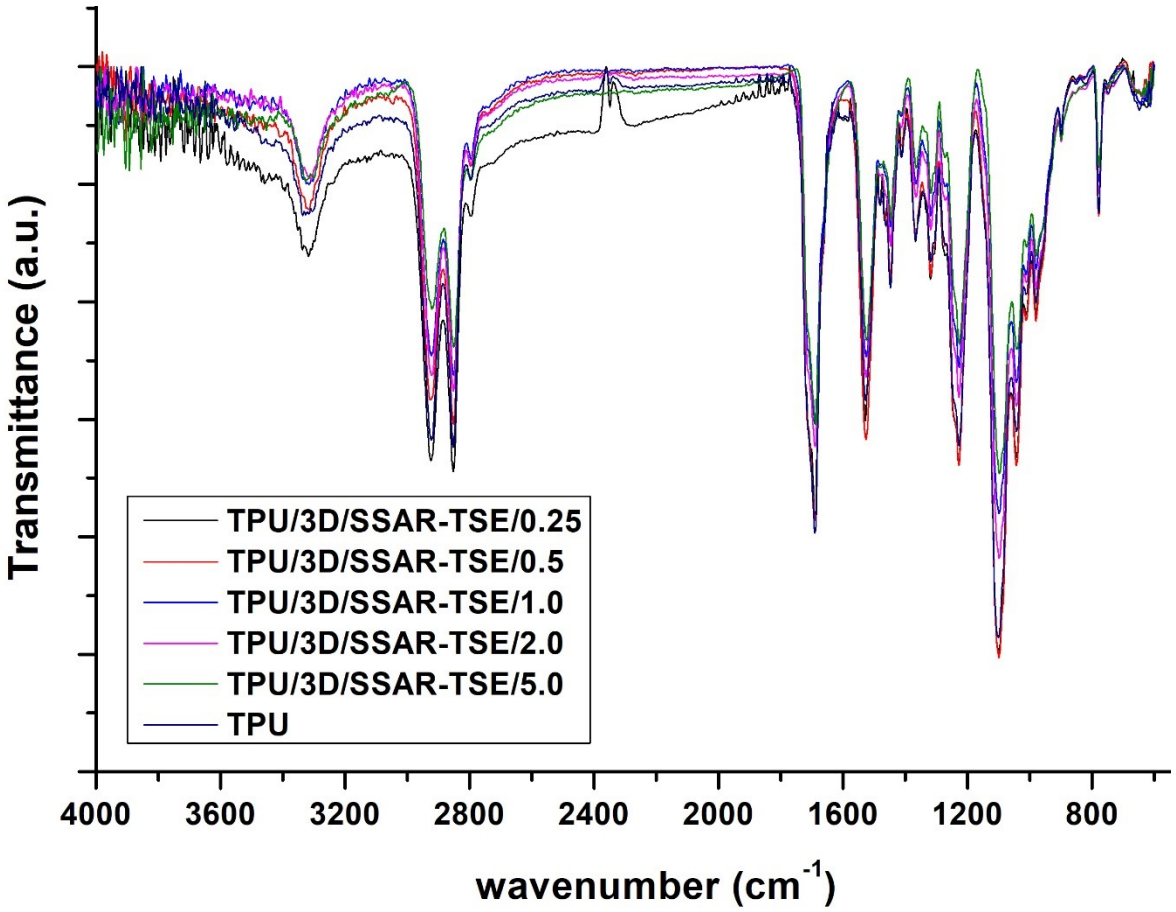

Figure S4: *ATR-FTIR spectra of neat thermoplastic polyurethane (TPU, navy blue color); polyurethane nanocomposite films reinforced with 0.25 wt% (TPU/3D/SSAR-TSE/0.25, black color), 0.5 wt% (TPU/3D/SSAR-TSE/0.5, red color), 1.0 wt% (TPU/3D/SSAR-TSE/1.0, blue color), 2 wt% (TPU/3D/SSAR-TSE/2.0, magenta color) and 5 wt% (TPU/3D/SSAR-TSE/5.0, green color) hybrid 3D nanofillers through SSAR followed by TSE in the range 4000-600 cm^{-1}.*

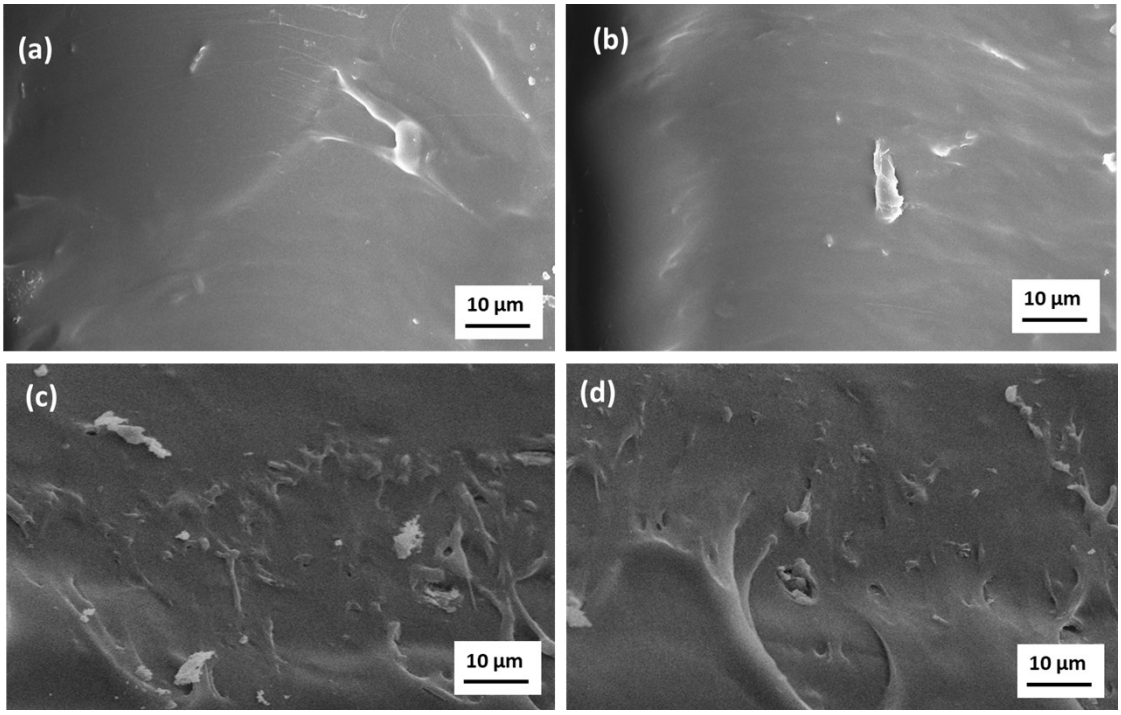

Figure S5: *SEM images of polyurethane nanocomposite films reinforced with hybrid 3D nanofiller of (a) 0.25 wt% and (b) 0.5 wt% by TSE; (c) 0.25 wt% and (d) 0.5 wt% through SSAR followed by TSE technique.*

References:

[1] P. Chamoli, M.K. Das, K.K. Kar, Green synthesis of silver-graphene nanocomposite based transparent conducting film, Phys. E: Low-dimens. Syst. Nanostruct. 90 (2017) 76-84. https://doi.org/10.1016/j.physe.2017.03.015.

[2] A. Hiltner, R.Y.F. Liu, Y.S. Hu, E. Baer. Oxygen transport as a solid-state structure probe for polymeric materials: A review, J. Polym. Sci. Part. B: Polym. Phys. 43 (2005) 1047–63. doi:10.1002/polb.20349.

[3] L.J. Van Rooyen, J. Karger-Kocsis, L. David Kock, Improving the helium gas barrier properties of epoxy coatings through the incorporation of graphene nanoplatelets and the influence of preparation techniques, J. Appl. Polym. Sci. 132(39) (2015). https://doi.org/10.1002/app.42584

[4] S. Mangaraj, T.K. Goswami, D.K. Panda. Modeling of gas transmission properties of polymeric films used for MA packaging of fruits, J. Food. Sci. Technol. 52 (2015) 5456–69. doi:10.1007/s13197-014-1682-2.

[5] Y. Nakano, T. Yanase, T. Nagahama, H. Yoshida, T. Shimada, Accurate and stable equal-pressure measurements of water vapor transmission rate reaching the 10^{-6} g m^{-2} day^{-1} range, Sci. Rep. 6 (2016) 35408;6. doi:10.1038/srep35408.

[6] K. Madhavan, B.S.R. Reddy, Poly(dimethylsiloxane-urethane) membranes: Effect of hard segment in urethane on gas transport properties, J. Memb. Sci. 283 (2006) 357–65. doi:10.1016/j.memsci.2006.07.005.

[7] F. Guo, G. Silverberg, S. Bowers, S.P. Kim, D. Datta, V. Shenoy, Graphene-based environmental barriers, Environ. Sci. Technol. 14 (2012) 7717-7724. https://doi.org/10.1021/ es301377y.

[8] J.D. Edwards, S.F. Pickering, Permeability of rubber to gases, J. Franklin. Inst. 190 (920) 253–4. doi:10.1016/S0016-0032(20)92050-1.

[9] J.G. Wijmans, R.W. Baker, The solution-diffusion model : a review, J. Memb. Sci. 107 (1995) 1–21. doi:10.1016/0376-7388(95)00102-I.

[10] M. Joshi, K. Banerjee, Polymer/clay nanocomposite based coatings for enhanced gas barrier property, Indian J. Fibre Text. Res. 3 (2006) 202–14. http://nopr.niscpr.res.in/handle/123456789/24507

[11] G.L. Robertson, Food Packaging: Principles and Practice, 3rd ed. Boca Raton: CRC Press, Taylor & Francis Group, 2012. doi:10.1177/0340035206070163.

[12] V. Siracusa, Food packaging permeability behaviour: A report, Int. J. Polym. Sci. 2012 (2012). doi:10.1155/2012/302029.

[13] E. Wicke, R. Kallenbach, Die Oberflächendiffusion von Kohlendioxyd in aktiven Kohlen. Kolloid-Zeitschrift, 97 (1941) 135–51. doi:10.1007/BF01502640.

[14] A.R. Manninen, H.E. Naguib, A.V. Nawaby, M. Day, CO2 sorption and diffusion in polymethyl methacrylateclay nanocomposites, Polym. Eng. Sci. 45 (2005) 904–14. doi:10.1002/pen.20350.

[15] D.M. Eitzman, R.R. Melkote, E.L. Cussler, Barrier membranes with tipped impermeable flakes, AIChE J. 42 (1996) 2–9. doi:10.1002/aic.690420103.

[16] W.R. Falla, M. Mulski, E.L. Cussler, Estimating diffusion through flake-filled membranes, J. Memb. Sci. 119 (1996) 129–38. doi:10.1016/0376-7388(96)00106-8.

[17] R. Aris, On a problem in hindered diffusion, Arch. Ration. Mech. Anal. 95 (1986) 83–91. doi:10.1007/BF00281082.

[18] W.A. Wakeham, E.A. Mason, Diffusion through Multiperforate Laminae, Ind. Eng. Chem. Fundam. 18 (1979) 301–5. doi:10.1021/i160072a001.

[19] N.K. Lape, E.E. Nuxoll, E.L. Cussler, Polydisperse flakes in barrier films, J. Memb. Sci. 236 (2004) 29–37. doi:10.1016/j.memsci.2003.12.026.

[20] G.H. Fredrickson, J. Bicerano, Barrier properties of oriented disk composites, J. Chem. Phys. 110 (1999) 2181–8. doi:10.1063/1.477829.

[21] Y. Cui, S.I. Kundalwal, S. Kumar, Gas barrier performance of graphene/polymer nanocomposites, Carbon 98 (2016) 313–33. doi:10.1016/j.carbon.2015.11.018.

[22] A.A. Gusev, H.R. Lusti, Rational design of nanocomposites for barrier applications, Adv. Mater. 13 (2001) 1641–3. doi:10.1002/1521-4095(200111)13:21<1641::AID-ADMA1641>3.0.CO;2-P.

[23] C. Lu, Y.W. Mai, Permeability modelling of polymer-layered silicate nanocomposites, Compos. Sci. Technol. 67 (2007) 2895–902. doi:10.1016/j.compscitech.2007.05.008.

[24] R.K. Bharadwaj, Modeling the barrier properties of polymer-layered silicate nanocomposites, Macromolecules 34 (2001) 9189–92. doi:10.1021/ma010780b.

[25] T. Bansala, M. Joshi, S. Mukhopadhyay, R.A. Doong, M. Chaudhary, Electrically conducting graphene-based polyurethane nanocomposites for microwave shielding applications in the Ku band, J. Mater. Sci. 52 (2017) 1546-1560. https://doi.org/10.1007/s10853-016-0449-8.

[26] R.D. Maksimov, S. Gaidukov, J. Zicans, J. Jansons, Moisture permeability of a polymer nanocomposite containing unmodified clay, Mech. Compos. Mater. 44 (2008) 505–14. doi:10.1007/s11029-008-9041-x.

[27] A. Sorrentino, M. Tortora, V. Vittoria, Diffusion behavior in polymer-clay nanocomposites, J. Polym. Sci. Part B: Polym. Phys. 44 (2006) 265–74. doi:10.1002/polb.20684.

[28] J.M. Herrera-Alonso, E. Marand, J.C. Little, S.S. Cox, Transport properties in PU/clay nanocomposites as barrier materials: Effect of processing conditions, J. Memb. Sci. 337 (2009) 208–14. doi:10.1016/j.memsci.2009.03.045.

[29] S. Nazarenko, P. Meneghetti, P. Julmon, B.G. Olson, S. Qutubuddin, Gas barrier of polystyrene montmorillonite clay nanocomposites: Effect of mineral layer aggregation, J. Polym. Sci. Part B: Polym. Phys. 45 (2007) 1733–53. doi:10.1002/polb.21181.